A localized view on molecular dissociation via electron-ion partial covariance

Felix Allum,[*,†] Valerija Music,[‡,¶] Ludger Inhester,[*,§] Rebecca Boll,[¶] Benjamin Erk,[‖] Philipp Schmidt,[‡,¶] Thomas M. Baumann,[¶] Günter Brenner,[‖] Michael Burt,[†] Philipp Demekhin,[‡] Simon Dörner,[‖] Arno Ehresmann,[‡] Andreas Galler,[¶] Patrik Grychtol,[¶] David Heathcote,[†] Denis Kargin,[⊥] Mats Larsson,[#] Jason W L Lee,[†,‖] Zheng Li,[§,@] Bastian Manschwetus,[‖] Lutz Marder,[‡] Robert Mason,[†] Michael Meyer,[¶] Huda Otto,[‡] Christopher Passow,[‖] Rudolf Pietschnig,[⊥] Daniel Ramm,[‖] Daniel Rolles,[△] Kaja Schubert,[‖] Lucas Schwob,[‖] Richard Thomas,[#] Claire Vallance,[†] Igor Vidanović,[⊥] Clemens von Korff Schmising,[▽] René Wagner,[¶] Peter Walter,[††] Vitali Zhaunerchyk,[‡‡] Sadia Bari,[‖] Mark Brouard,[†] and Markus Ilchen[*,‖,‡,¶]

†*The Chemistry Research Laboratory, Department of Chemistry, University of Oxford, Oxford OX1 3TA, United Kingdom*

‡*Institut für Physik und CINSaT, Universität Kassel, Heinrich-Plett-Straße 40, D-34132 Kassel, Germany*

¶*European XFEL GmbH, Holzkoppel 4, 22869 Schenefeld, Germany*

§*Center for Free-Electron Laser Science CFEL, Deutsches Elektronen-Synchrotron DESY, Notkestraße 85, 22607 Hamburg, Germany*

‖*Deutsches Elektronen-Synchrotron DESY, Notkestraße 85, 22607 Hamburg, Germany*

⊥*Institut für Chemie, Universität Kassel, Heinrich-Plett-Straße 40, D-34132 Kassel, Germany*

#*University of Stockholm, Alba Nova Institute, Roslagstullsbacken 21, 114 21 Stockholm, Sweden*

@*State Key Laboratory for Mesoscopic Physics, School of Physics, Peking University, Beijing 100871, China*

△*Kansas State University, 1228 N 17th St, KS 66506, United States of America*

▽*Max Born Institute, Max-Born-Straße 2A, 12489 Berlin, Germany*

††*SLAC National Accelerator Laboratory, 2575 Sand Hill Road, Menlo Park, California 94025, USA*

‡‡*University of Gothenburg, 405 30 Gothenburg, Sweden*

E-mail: felix.allum@chem.ox.ac.uk; ludger.inhester@desy.de; markus.ilchen@desy.de

Abstract

Inner-shell photoelectron spectroscopy provides an element-specific probe of molecular structure, as core-electron binding energies are sensitive to the chemical environment. Short-wavelength femtosecond light sources, such as Free-Electron Lasers (FELs), even enable time-resolved site-specific investigations of molecular photochemistry. Here, we study the ultraviolet photodissociation of chiral (R/S)-1-iodo-2-methylbutane, probed by XUV pulses from the Free-electron LASer in Hamburg (FLASH) through the ultrafast evolution of the iodine 4d binding energy. Methodologically, we introduce electron-ion partial covariance imaging as a technique to isolate otherwise elusive features in a two-dimensional photoelectron spectrum arising from different photofragmentation pathways. The experimental and theoretical results for the time-resolved electron spectra of the $4d_{3/2}$ and $4d_{5/2}$ atomic and molecular levels that are disentangled by this method provide a key step towards studying structural and chemical changes from a specific spectator site. We thus pave the way for approaching femto-stereochemistry with FELs.

Graphical TOC Entry

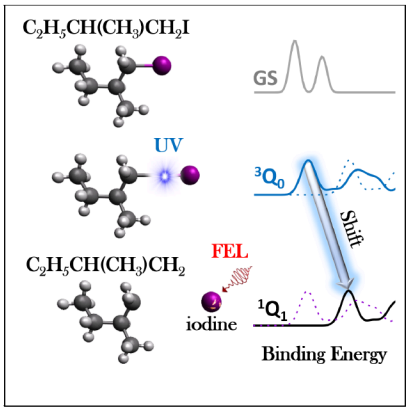

Molecular restructuring and its consequences for molecular function are of ubiquitous interest across a variety of scientific disciplines. The physical and chemical dynamics involved typically progress on the femtosecond timescale, enabling their 'real-time' observation through a range of ultrafast spectroscopic techniques.[1] Modern technological developments in high intensity short-wavelength FELs have extended such methods for probing ultrafast chemistry in a site-selective manner by utilizing wavelengths of light which can selectively address core orbitals.[2–9]

Ultrafast molecular fragmentation can cause significant core-electron binding energy changes. These changes are on the order of few eV for chemical shifts of neutral fragments, tens of eV for delocalized charges in the valence shell and more than a hundred eV for localized core-holes.[10] Such shifts are measurable by photoelectron spectroscopy,[5–7] but it is difficult to distinguish smaller shifts from static signal originating from ground-state molecules and background.[7] Additionally, relating such signal to a specific underlying process is challenging, particularly in the case of more complex molecules which may undergo a range of photochemical processes following photoexcitation. One potential solution is to utilize electron-ion correlations, allowing electron spectroscopy to be applied in a channel-resolved manner, by isolating contributions in an electron spectrum correlated to a specific photofragmentation channel, determined by ion spectroscopy.[11–13] Electron-ion coincidence techniques have proven to be very powerful, but are limited to very low count rates, such that multiple particles produced in the same laser pulse can be assigned to a single event.[14,15] While progress in coincidence experiments at FELs has been made,[2,9,16–18] the high repetition rates required for sufficient data collection still pose a considerable technical challenge that can prospectively be tackled by high-repetition rate FELs.[19] Here, we exploit an alternative method to determine charged-particle correlations at far higher count rates; through calculating the covariance, a measure of linear correlation between the signals of interest recorded over many data acquisition cycles (i.e. laser shots).[20,21] This holds the promise of being applicable even to larger molecules.[22] Although the inherently unstable conditions due

to stochastic pulse generation at Self-Amplified Spontaneous Emission (SASE) FELs provide challenges for correlation techniques, schemes have been developed to not only correct for the adverse effects of such fluctuations, but effectively exploit them through either partial[23,24] or contingent[25] covariance analysis. In the present work, we demonstrate the extension of these techniques, usually applied to a 1D mass spectrum, to a 3D Velocity-Map Imaging (VMI) study of the ultrafast evolution of electronic structure during a photodissociation, at a particular core site, in a channel-resolved manner.

The prototypical chiral molecule 1-iodo-2-methylbutane ($C_2H_5CH\,(CH_3)CH_2I$) is a prominent candidate for approaching dynamical investigations of chirality with FELs. Understanding and benchmarking the underlying ultrafast photochemistry is an important prerequisite for these kind of studies. Here, it is dissociated at its C-I bond following single-photon UV excitation. The subsequently evolving chemical dynamics are investigated from the viewpoint of the released neutral iodine atom via a time-delayed, $\sim$63.5 eV, FEL-based probe pulse with $\sim$50 fs duration. Due to the large cross-section differences, the I 4d orbital is predominantly ionized.[26] By using covariance analysis to select only electrons that are emitted from neutrally dissociated iodine, and following their time evolution during the photolysis, an advanced scheme for femtochemistry is enabled via simultaneous electron and ion VMI spectroscopy.[27–30] The interpretation of the delay-dependent photoelectron spectra is supported by state-of-the-art simulations of photoionization.[31]

Figure 1a) shows mass spectra of 1-iodo-2-methylbutane exposed to the UV and XUV pulses alone, or with both pulses for positive pump-probe delays (UV preceding the XUV). At the employed intensities, very little multi-photon dissociative ionization is initiated by the UV pulse alone, whereas the XUV pulse causes extensive ionic break-up. In the two-color experiment, a clear pump-probe signal can be observed most prominently in the I^{2+} ion, whose yield is significantly enhanced when the UV pulse precedes the XUV. As ionization at the I 4d orbital by the XUV predominantly results in two charges after Auger decay,[26] UV-induced neutral photodissociation followed by ionization at the nascent iodine atoms by

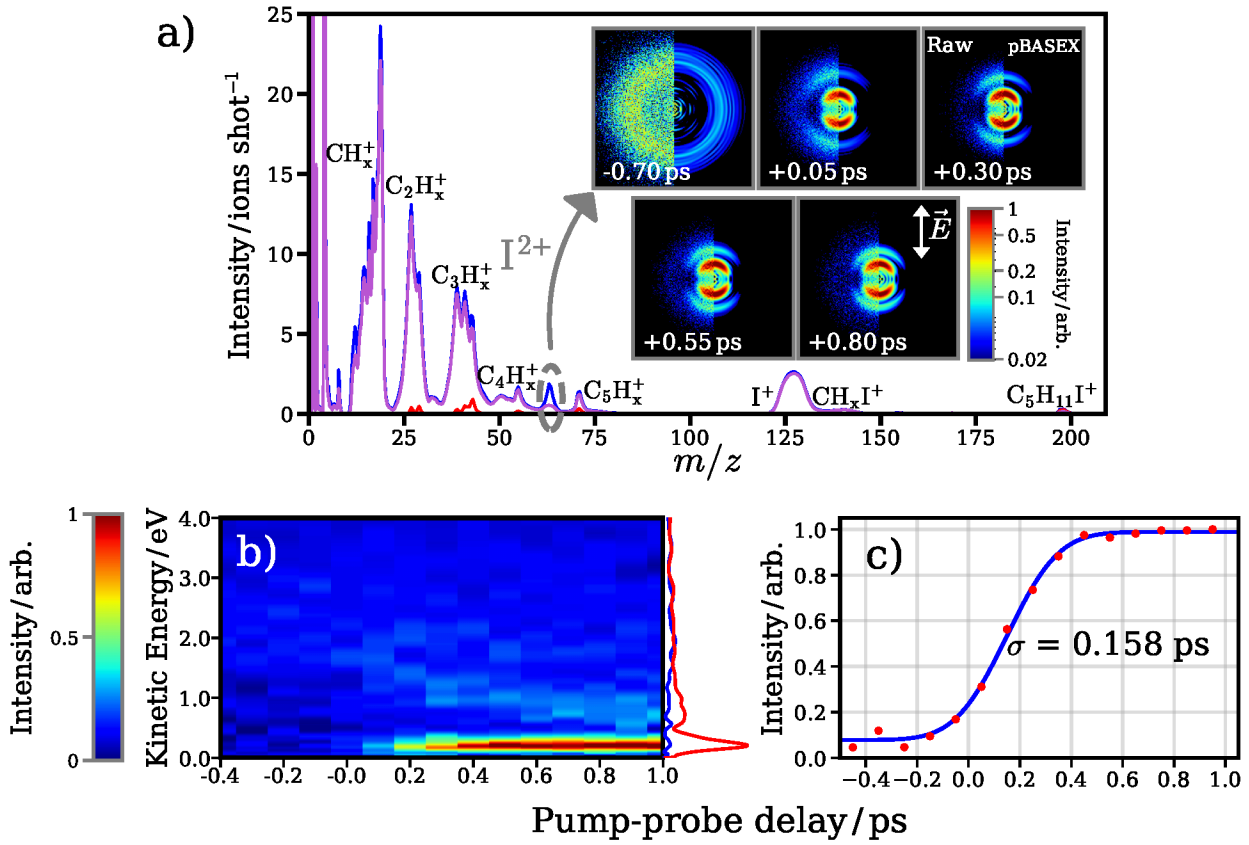

Figure 1: a) Normalized ion mass spectra recorded for 1-iodo-2-methylbutane with the XUV only (magenta), UV only (red) and UV early-XUV late (blue). Inset: Raw (left) and reconstructed (right)[32] velocity-map I^{2+} ion images at a series of pump-probe delays. The -0.70 ps image's intensity has been multiplied by 5, to increase the visibility of the weak, high-KER channel. b) Delay-dependent kinetic energy distribution for the I^{2+} ion. The UV-early (>1 ps delay) and UV late (<-0.2 ps delay) distributions are projected in red and blue respectively. c) Integrated yield of the low kinetic energy (<0.4 eV) feature as a function of pump-probe delay (red points) with a fit to a normal CDF (blue line).

the XUV would lead to an enhanced I^{2+} signal at sufficiently large internuclear distances, for which charge transfer does not occur.[3] Small enhancements of other fragments are also visible in comparison to the XUV-only spectrum.

Velocity-map images for the I^{2+} ion at a series of pump-probe delays, shown in the inset of Figure 1a), provide insight into the UV-induced C-I dissociation. At negative pump-probe delays (UV late), a weak, broad feature at high radii is observed, that is assigned to a (multi-photon) XUV-induced Coulomb explosion of the parent molecule. When the UV pulse pre-excites the molecules, two clear features emerge in the ion images. Firstly, there is a strong contribution at low radii, which is peaked along the UV polarization axis ($\beta \approx 1.80$). This is expected for neutral photodissociation following a parallel excitation predominantly to the $^3Q_0$ state, as observed in similar alkyl iodides.[33] The delay-dependent I^{2+} kinetic energy is plotted in Figure 1b), and panel c) shows the integrated intensity of the low kinetic energy, neutral dissociation feature.

Secondly, a weaker, more diffuse feature at higher radii is also visible after time-zero. This moves towards the center of the image at longer pump-probe delays, indicative of a Coulombic contribution to the fragment energy, which decreases at larger internuclear separations, i.e. longer pump-probe delays.[3,4,34] Covariance imaging analysis[34–37] confirms that this minor channel arises from a multi-photon dissociative ionization by the pump pulse, prior to XUV absorption at the iodine site, and is not discussed further in this work, which focuses on the dominant, neutral photodissociation channel.

The photodissociation dynamics can be further probed through time-resolved inner-shell photoelectron spectroscopy[5–7,31] at the iodine 4d site, as demonstrated on the ultraviolet photodissociation of methyl iodide by Braußе *et al.*,[7] in which a small increase in I 4d binding energy was detected following UV excitation. This was assigned to ionization of dissociated iodine atoms, supported by earlier synchrotron measurements of the I 4d binding energies of CH_3I and I.[38–41] The ability to study the temporal evolution of the signal, however, was hampered by the fact that this small contribution overlaps energetically with signal

arising from unpumped parent molecules (due in part to the significant FEL bandwidth); a limitation that can be tackled by the partial covariance analysis. A primary aspect of the current work is that this method can be utilized to isolate delay-dependent spectral features of interest.

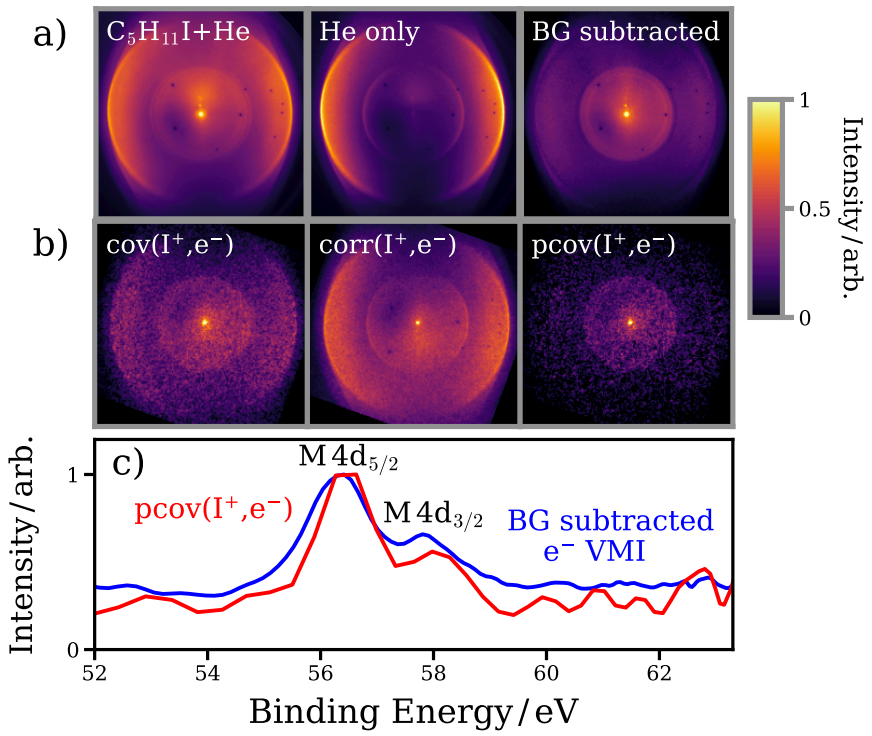

Figure 2: a) Photoelectron VMI images (UV-XUV) of: (left to right) 1-iodo-2-methylbutane seeded in He carrier gas, He only and 1-iodo-2-methylbutane following background subtraction. b) Electron-ion partial covariance analysis for the I^+ ion, showing images of (left to right) covariance, correction term and the partial covariance. c) Electron spectra associated with the background subtracted velocity-map electron image (blue) and the I^+ electron-ion partial covariance image (red). The two main features, arising from molecular $4d_{5/2}$ and $4d_{3/2}$ ionization, are labelled.

Photoelectron images following irradiation of 1-iodo-2-methylbutane (seeded in He) by the UV and XUV lasers are plotted in Figure 2a). The strong rings observed in the helium-only case are due to single and double ionization of He by the XUV pulse, which form a significant background when 1-iodo-2-methylbutane is present, labelled '$C_5H_{11}I$' in Figure 2a). Subtraction of background contributions yields the image plotted on the right of panel

a) of Figure 2. A feature at slightly lower kinetic energy (higher binding energy) than the He^{2+} photoline is observed, arising from ionization at the I 4d site in $C_5H_{11}I$. The associated electron binding energy spectrum (Figure 2c)) shows two clear peaks at approximately 56.5 eV and 58 eV, which can be assigned to the molecular $4d_{5/2}$ and $4d_{3/2}$ levels, respectively. The β_2 parameter[42] for electrons originating from the molecular I 4d site was determined to be $\beta_2 = 0.25$ for the $4d_{5/2}$ and $\beta_2 = 0.3$ for the $4d_{3/2}$, which is in reasonable agreement to previous work on CH_3I[43] under the given experimental conditions.

The electron velocity distributions correlated with production of a particular photoion can be extracted by calculating the covariance between the integrated count of the ion of interest and each pixel of the electron image. As three-dimensional ion-velocity information is recorded, electron spectra correlated to a specific range of ion velocities can be calculated by appropriately selecting ions within a given velocity range. Figure 2b) shows the electron-ion covariance calculated for the I^+ ion, which is predominantly produced following interaction of the molecule with the XUV pulse alone. The I 4d photoline is clearly highlighted in this covariance image, however there is still significant background present from the He seeding gas. This 'false' covariance is attributed to correlations induced by the fluctuating FEL power during the experiment, which can be accounted for through partial covariance analysis[23,24,44] (details of the partial covariance procedure are given in the Supporting Information). An additional map, denoted the 'correction' map, representing the (linear) correlations induced by the fluctuating FEL pulse energy is constructed. Subtraction of this term from the covariance term yields the partial covariance, which isolates the true electron-ion correlations. In panel c), strong principal agreement is observed between the covariant electron spectrum for I^+ and the equivalent spectrum obtained following subtraction of the various background contributions from the raw electron image.

As discussed previously, the low kinetic energy I^{2+} ions observed in Figure 1 are formed by a distinct pathway: UV-induced photodissociation and subsequent XUV ionization at the nascent iodine atom 4d orbital. The partial covariance image for low-velocity I^{2+} ions is

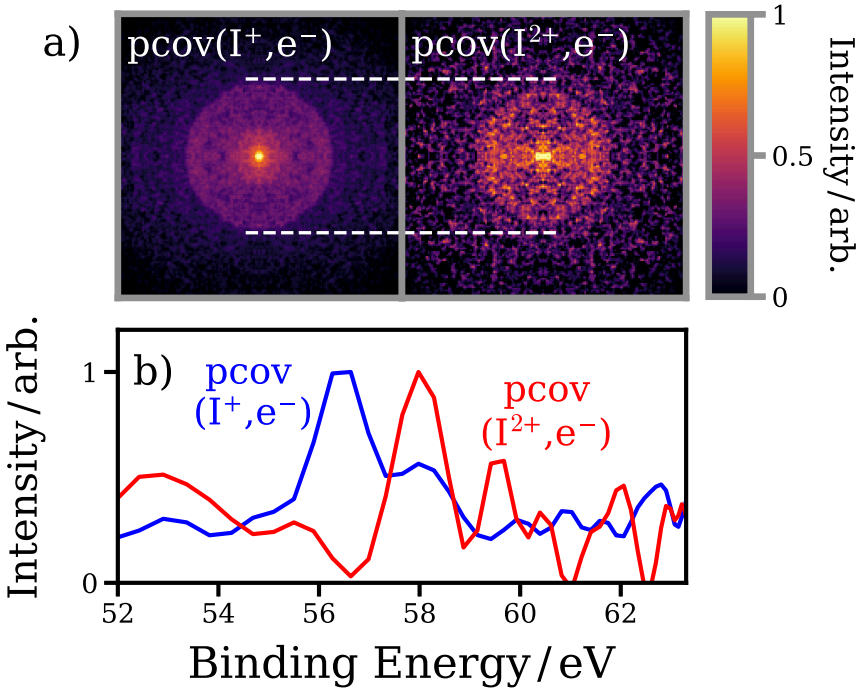

Figure 3: a) Electron-ion partial covariance images (symmetrized) for the I^+ ion and the I^{2+} ion (low radius ions only, for pump-probe delays of +0.55 ps and +0.80 ps). A horizontal line at the radius of the ring seen in the I^+ image highlights the shift to lower radius in the I^{2+} case. b) Photoelectron spectra extracted from each of these partial covariance images.

plotted in Figure 3a), for long positive pump-probe delays (UV first by at least 550 fs). In Figure 1a)), a clear circular feature is observed at a significantly lower radius (higher electron binding energy) than for XUV-only ionization and fragmentation of the parent molecule. As seen in Figure 3b), the spectrum associated with the neutral dissociation exhibits a shift to higher binding energies, by approximately 1.5 - 2 eV, consistent with synchrotron studies on the I 4d photoelectron spectra of free iodine atoms.[39,40] Crucially, and in contrast to previous work,[7] this energetic shift as a result of dissociation can be completely isolated from the far stronger unpumped parent molecule signal in the present case, as well as from any competing pump-probe channels, such as the multiphoton dissociative ionization pathway. As such, the here presented method allows for decisive insights into the photochemistry of the chosen prototypical chiral molecule.

The covariant electron spectra associated with low-velocity I^{2+} ions can be calculated in a time-resolved manner, as shown in Figure 4. For all pump-probe delays, the electron spectra in covariance with the I^{2+} photodissociation products show clear differences from the spectrum of ground state molecules. Three main peaks can be seen in these spectra in the ∼56 - 61 eV region, along with an immediate, unresolved, shift to higher electron binding energies. In the ∼54-56 eV region, the weak signal is assigned to the partial covariance routine failing to remove all the He-background contributions.

In order to better understand the origins of these experimental observations, we have calculated photoelectron spectra as a function of carbon-iodine distance keeping the remaining geometry parameters fixed, for the $^3Q_0$ and $^1Q_1$ excited states (a full description of the theoretical methods is given in the Supporting Information). As in CH_3I and other iodoalkanes,[45–47] photoexcitation occurs predominantly to the $^3Q_0$ state, which correlates to spin-orbit excited I^* ($^2P_{1/2}$) products.[48] This state is crossed by the $^1Q_1$ state, in our case at around 2.4 Å C-I bond distance, correlating to ground state I ($^2P_{3/2}$). From our simulations of the C-I bond elongation, which reaches an asymptotic velocity of ∼25 Å ps^{-1}, this channel-crossing occurs after a few tens of fs. During the dissociation, significant population transfer

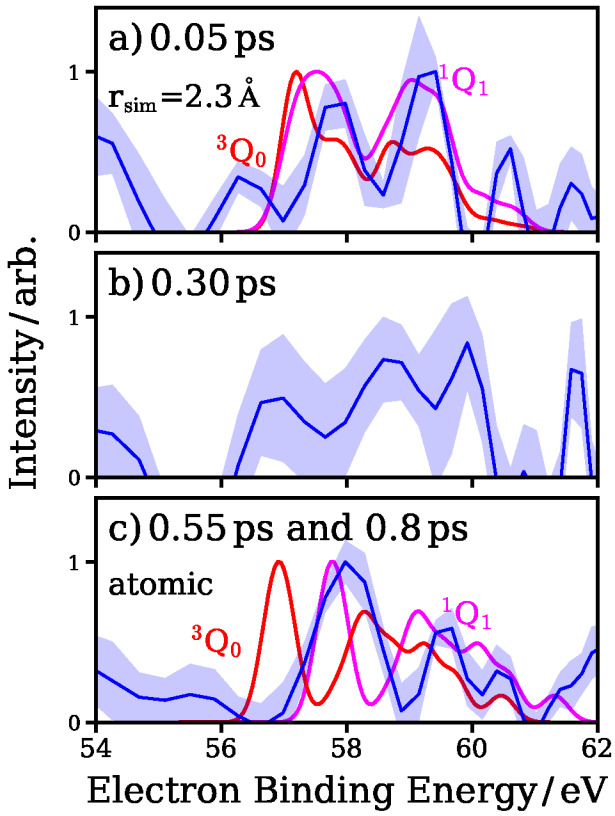

Figure 4: a) to c): Angle-integrated electron spectra extracted from the I^{2+} electron-ion partial covariance images at a series of pump-probe delays (blue). For each spectrum, the shaded area represents errors at the 1σ level estimated from a bootstrapping analysis. In panels a) and c), simulated spectra on the $^3Q_0$ (red) and $^1Q_1$ (magenta) potentials are shown. In panel a), this is for a for C-I bond distance of 2.30 Å, whereas in b), the theoretical spectra are in the dissociated (i.e. atomic) limits.

from $^3Q_0$ to $^1Q_1$ occurs enabling production of ground state I atoms. This is the dominant dissociation pathway, particularly in larger alkyl iodides.[33,49] In Figure 4, the time-resolved experimental data are compared with theoretical spectra calculated close to the equilibrium bond distance (panel a)), and in the long bond distance limit (panel c)) for both states.

Although the time resolution of ±100 fs precludes direct observation of the non-adiabatic behavior at the conical intersection,[49,50] the comparison with theory is still illuminating. At the earliest pump-probe delay, potential contributions from the initially populated $^3Q_0$ state and the $^1Q_1$ state cannot be clearly distinguished, with qualitative indications for either state, consistent with some convolution of both involved states. For the second delay at 300 fs, the evolution of the spectral dynamics (primarly on the $^1Q_1$ state) is theoretically predicted to be concluded, which cannot be decisively confirmed by the present data. For long delays, in contrast, the dominant contribution can be clearly assigned to the $^1Q_1$ channel ($I(^2P_{3/2})$), with any minor contributions from the $^3Q_0$ state causing a significantly smaller binding energy shift than that observed.

The current work demonstrates the applicability of electron-ion partial covariance imaging to ultrafast site-specific photoelectron spectroscopy. Future upgrades to FELs in terms of repetition rate, polarization[51] and pulse duration[52] control, in combination with ultrashort optical laser pulses in particular in the UV regime,[53–55] and advanced camera readout schemes, will enhance the data acquisition rates by orders of magnitude. Experiments building on this methodology presented here will enable the study of coupled nuclear electron dynamics, such as those associated with conical intersections, in exquisite detail. Besides gaining first photochemical insights into the chiral molecule 1-iodo-2-methylbutane, our approach can also be readily extended to asymmetric angular distributions, in either the laboratory- or recoil-frame which provides a promising tool for exploring ultrafast *chiral* dynamics.

Acknowledgement

We gratefully acknowledge DESY for provision of the free-electron laser beamtime at the BL1 CAMP endstation of FLASH as well as the work and sedulous support of the scientific and technical teams. FA, MB, DH, RM and CV acknowledge funding from EPSRC Programme Grants EP/L005913/1 and EP/T021675/1. M. Bu is grateful for support from the UK EPSRC (EP/S028617/1 and EP/L005913/1). This work was partly funded by the Deutsche Forschungsgemeinschaft (DFG)–Project No. 328961117–SFB 1319 ELCH (Extreme light for sensing and driving molecular chirality). We furthermore acknowledge the Max Planck Society for funding the development and the initial operation of the CAMP end-station within the Max Planck Advanced Study Group at CFEL and for providing this equipment for CAMP@FLASH. The installation of CAMP@FLASH was partially funded by the BMBF grants 05K10KT2, 05K13KT2, 05K16KT3 and 05K10KTB from FSP-302. MI, VM, and PhS acknowledge funding by the Volkswagen Foundation within a Peter-Paul-Ewald Fellowship. SD, KS, LS, and SB acknowledge funding from the Helmholtz Initiative and Networking Fund through the Young Investigators Group Program (VH-NG-1104). Furthermore, KS and SB were supported by the Deutsche Forschungsgemeinschaft, project B03 in the SFB 755 - Nanoscale Photonic Imaging. DR was supported by the US National Science Foundation through grant PHYS-1753324.

Supporting Information Available

Experimental methods; theoretical methods; assignment of time-zero; estimation of experimental errors; details of the electron-ion partial covariance calculation

References

(1) Zewail, A. H. Femtochemistry: Atomic-Scale Dynamics of the Chemical Bond. *J. Phys. Chem. A* **2000**, *104*, 5660–5694.

(2) Erk, B.; Rolles, D.; Foucar, L.; Rudek, B.; Epp, S. W.; Cryle, M.; Bostedt, C.; Schorb, S.; Bozek, J.; Rouzee, A. et al. Inner-shell multiple ionization of polyatomic molecules with an intense x-ray free-electron laser studied by coincident ion momentum imaging. *J. Phys. B At. Mol. Opt. Phys.* **2013**, *46*, 164031.

(3) Erk, B.; Boll, R.; Trippel, S.; Anielski, D.; Foucar, L.; Rudek, B.; Epp, S. W.; Coffee, R.; Carron, S.; Schorb, S. et al. Imaging charge transfer in iodomethane upon x-ray photoabsorption. *Science* **2014**, *345*, 288–291.

(4) Boll, R.; Erk, B.; Coffee, R.; Trippel, S.; Kierspel, T.; Bomme, C.; Bozek, J. D.; Burkett, M.; Carron, S.; Ferguson, K. R. et al. Charge transfer in dissociating iodomethane and fluoromethane molecules ionized by intense femtosecond X-ray pulses. *Structural Dynamics* **2016**, *3*, 043207.

(5) Wernet, P.; Leitner, T.; Josefsson, I.; Mazza, T.; Miedema, P. S.; Schröder, H.; Beye, M.; Kunnus, K.; Schreck, S.; Radcliffe, P. et al. Communication: Direct evidence for sequential dissociation of gas-phase $Fe(CO)_5$ via a singlet pathway upon excitation at 266 nm. *J. Chem. Phys.* **2017**, *146*, 211103.

(6) Leitner, T.; Josefsson, I.; Mazza, T.; Miedema, P. S.; Schröder, H.; Beye, M.; Kunnus, K.; Schreck, S.; Düsterer, S.; Föhlisch, A. et al. Time-resolved electron spectroscopy for chemical analysis of photodissociation: Photoelectron spectra of $Fe(CO)_5$, $Fe(CO)_4$, and $Fe(CO)_3$. *J. Chem. Phys.* **2018**, *149*, 044307.

(7) Braußе, F.; Goldsztejn, G.; Amini, K.; Boll, R.; Bari, S.; Bomme, C.; Brouard, M.; Burt, M.; De Miranda, B. C.; Düsterer, S. et al. Time-resolved inner-shell photoelectron

spectroscopy: From a bound molecule to an isolated atom. *Phys. Rev. A* **2018**, *97*, 043429.

(8) Forbes, R.; Allum, F.; Bari, S.; Boll, R.; Brouard, M.; Bucksbaum, P.; Ekanayake, N.; Erk, B.; Howard, A.; Johnsson, P. et al. Time-resolved site-selective imaging of predissociation and charge transfer dynamics: the CH_3I B-band . *J. Phys. B At. Mol. Opt. Phys.* **2020**,

(9) Li, X.; Inhester, L.; Osipov, T.; Boll, R.; Coffee, R.; Cryan, J.; Gatton, A.; Gorkhover, T.; Hartman, G.; Ilchen, M. et al. Electron-ion coincidence measurements of molecular dynamics with intense X-ray pulses. *Scientific reports* **2021**, *11*, 1–12.

(10) Mazza, T.; Ilchen, M.; Kiselev, M. D.; Gryzlova, E. V.; Baumann, T. M.; Boll, R.; De Fanis, A.; Grychtol, P.; Montaño, J.; Music, V. et al. Mapping Resonance Structures in Transient Core-Ionized Atoms. *Phys. Rev. X* **2020**, *10*, 041056.

(11) Davies, J. A.; LeClaire, J. E.; Continetti, R. E.; Hayden, C. C. Femtosecond time-resolved photoelectron-photoion coincidence imaging studies of dissociation dynamics. *J. Chem. Phys.* **1999**, *111*, 1–4.

(12) Boguslavskiy, A. E.; Mikosch, J.; Gijsbertsen, A.; Spanner, M.; Patchkovskii, S.; Gador, N.; Vrakking, M. J.; Stolow, A. The multielectron ionization dynamics underlying attosecond strong-field spectroscopies. *Science* **2012**, *335*, 1336–1340.

(13) Forbes, R.; Boguslavskiy, A. E.; Wilkinson, I.; Underwood, J. G.; Stolow, A. Excited state wavepacket dynamics in NO_2 probed by strong-field ionization. *J. Chem. Phys.* **2017**, *147*, 054305.

(14) Continetti, R. E. Coincidence spectroscopy. *Annu. Rev. Phys. Chem.* **2001**, *52*, 165–192.

(15) Arion, T.; Hergenhahn, U. Coincidence spectroscopy: Past, present and perspectives. *Journal of Electron Spectroscopy and Related Phenomena* **2015**, *200*, 222–231.

(16) Schnorr, K.; Senftleben, A.; Kurka, M.; Rudenko, A.; Schmid, G.; Pfeifer, T.; Meyer, K.; Kübel, M.; Kling, M.; Jiang, Y. et al. Electron Rearrangement Dynamics in Dissociating I 2 n + Molecules Accessed by Extreme Ultraviolet Pump-Probe Experiments. *Phys. Rev. Lett.* **2014**, *113*, 073001.

(17) Kastirke, G.; Schöffler, M. S.; Weller, M.; Rist, J.; Boll, R.; Anders, N.; Baumann, T. M.; Eckart, S.; Erk, B.; De Fanis, A. et al. Double Core-Hole Generation in O_2 Molecules Using an X-Ray Free-Electron Laser: Molecular-Frame Photoelectron Angular Distributions. *Phys. Rev. Lett.* **2020**, *125*, 163201.

(18) Kastirke, G.; Schöffler, M. S.; Weller, M.; Rist, J.; Boll, R.; Anders, N.; Baumann, T. M.; Eckart, S.; Erk, B.; De Fanis, A. et al. Photoelectron Diffraction Imaging of a Molecular Breakup Using an X-Ray Free-Electron Laser. *Phys. Rev. X* **2020**, *10*, 021052.

(19) Decking, W.; Abeghyan, S.; Abramian, P.; Abramsky, A.; Aguirre, A.; Albrecht, C.; Alou, P.; Altarelli, M.; Altmann, P.; Amyan, K. et al. A MHz-repetition-rate hard X-ray free-electron laser driven by a superconducting linear accelerator. *Nature Photonics* **2020**, 1–7.

(20) Frasinski, L. J.; Codling, K.; Hatherly, P. A. Covariance Mapping: A Correlation Method Applied to Multiphoton Multiple Ionization. *Science* **1989**, *246*, 1029–1031.

(21) Frasinski, L. J. Covariance mapping techniques. *J. Phys. B* **2016**, *49*, 152004.

(22) Driver, T.; Cooper, B.; Ayers, R.; Pipkorn, R.; Patchkovskii, S.; Averbukh, V.; Klug, D. R.; Marangos, J. P.; Frasinski, L. J.; Edelson-Averbukh, M. Two-Dimensional Partial-Covariance Mass Spectrometry of Large Molecules Based on Fragment Correlations. *Physical Review X* **2020**, *10*, 041004.

(23) Kornilov, O.; Eckstein, M.; Rosenblatt, M.; Schulz, C. P.; Motomura, K.; Rouzée, A.; Klei, J.; Foucar, L.; Siano, M.; Lübcke, A. et al. Coulomb explosion of diatomic molecules in intense XUV fields mapped by partial covariance. *J. Phys. B At. Mol. Opt. Phys.* **2013**, *46*, 164028.

(24) Frasinski, L. J.; Zhaunerchyk, V.; Mucke, M.; Squibb, R. J.; Siano, M.; Eland, J. H.; Linusson, P.; V.d. Meulen, P.; Salén, P.; Thomas, R. D. et al. Dynamics of hollow atom formation in intense X-ray pulses probed by partial covariance mapping. *Phys. Rev. Lett.* **2013**, *111*, 073002.

(25) Zhaunerchyk, V.; Frasinski, L. J.; Eland, J. H.; Feifel, R. Theory and simulations of covariance mapping in multiple dimensions for data analysis in high-event-rate experiments. *Phys. Rev. A - At. Mol. Opt. Phys.* **2014**, *89*, 1–8.

(26) Olney, T. N.; Cooper, G.; Brion, C. E. Quantitative studies of the photoabsorption (4.5-488 eV) and photoionization (9-59.5 eV) of methyl iodide using dipole electron impact techniques. *Chem. Phys.* **1998**, *232*, 211–237.

(27) Eppink, A. T. J. B.; Parker, D. H. Velocity map imaging of ions and electrons using electrostatic lenses: Application in photoelectron and photofragment ion imaging of molecular oxygen. *Rev. Sci. Instrum.* **1997**, *68*, 3477–3484.

(28) Erk, B.; Müller, J. P.; Bomme, C.; Boll, R.; Brenner, G.; Chapman, H. N.; Correa, J.; Düsterer, S.; Dziarzhytski, S.; Eisebitt, S. et al. CAMP@FLASH: an end-station for imaging, electron- and ion-spectroscopy, and pump–probe experiments at the FLASH free-electron laser. *J. Synchrotron Radiat.* **2018**, *25*, 1529–1540.

(29) Nomerotski, A.; Adigun-Boaye, S.; Brouard, M.; Campbell, E.; Clark, A.; Crooks, J.; John, J.; Johnsen, A.; Slater, C.; Turchetta, R. et al. Pixel imaging mass spectrometry with fast silicon detectors. *Nucl. Instruments Methods Phys. Res. Sect. A Accel. Spectrometers, Detect. Assoc. Equip.* **2011**, *633*, S243–S246.

(30) John, J. J.; Brouard, M.; Clark, A.; Crooks, J.; Halford, E.; Hill, L.; Lee, J. W. L.; Nomerotski, A.; Pisarczyk, R.; Sedgwick, I. et al. PImMS, a fast event-triggered monolithic pixel detector with storage of multiple timestamps. *J. Instrum.* **2012**, *7*, C08001–C08001.

(31) Inhester, L.; Li, Z.; Zhu, X.; Medvedev, N.; Wolf, T. J. Spectroscopic Signature of Chemical Bond Dissociation Revealed by Calculated Core-Electron Spectra. *J. Phys. Chem. Lett.* **2019**, *10*, 6536–6544.

(32) Garcia, G. A.; Nahon, L.; Powis, I. Two-dimensional charged particle image inversion using a polar basis function expansion. *Rev. Sci. Instrum.* **2004**, *75*, 4989–4996.

(33) Corrales, M. E.; Loriot, V.; Balerdi, G.; González-Vázquez, J.; De Nalda, R.; Bañares, L.; Zewail, A. H. Structural dynamics effects on the ultrafast chemical bond cleavage of a photodissociation reaction. *Phys. Chem. Chem. Phys.* **2014**, *16*, 8812–8818.

(34) Allum, F.; Anders, N.; Brouard, M.; Bucksbaum, P. H.; Burt, M.; Downes-ward, B.; Grundmann, S.; Harries, J.; Ishimura, Y.; Iwayama, H. et al. Multi-channel photodissociation and XUV-induced charge transfer dynamics in strong-field-ionized methyl iodide studied with time-resolved recoil-frame covariance imaging. *Faraday Discuss.* **2020**,

(35) Slater, C. S.; Blake, S.; Brouard, M.; Lauer, A.; Vallance, C.; John, J. J.; Turchetta, R.; Nomerotski, A.; Christensen, L.; Nielsen, J. H. et al. Covariance imaging experiments using a pixel-imaging mass-spectrometry camera. *Phys. Rev. A* **2014**, *89*, 011401.

(36) Slater, C. S.; Blake, S.; Brouard, M.; Lauer, A.; Vallance, C.; Bohun, C. S.; Christensen, L.; Nielsen, J. H.; Johansson, M. P.; Stapelfeldt, H. Coulomb-explosion imaging using a pixel-imaging mass-spectrometry camera. *Phys. Rev. A* **2015**, *91*, 053424.

(37) Allum, F.; Burt, M.; Amini, K.; Boll, R.; Köckert, H.; Olshin, P. K.; Bari, S.;

Bomme, C.; Braußе, F.; Cunha de Miranda, B. et al. Coulomb explosion imaging of CH_3I and CH_2ClI photodissociation dynamics. *J. Chem. Phys.* **2018**, *149*, 204313.

(38) Carlson, T. A.; Fahlman, A.; Krause, M. O.; Keller, P. R.; Taylor, J. W.; Whitley, T.; Grimm, F. A. Angle resolved photoelectron spectroscopy of the valence shells in HI and CH_3I as a function of photon energy from 13 to 90 eV. *J. Chem. Phys.* **1984**, *80*, 3521–3527.

(39) Tremblay, J.; Larzilliere, M.; Combet-Farnoux, F.; Morin, P. Photoelectron spectroscopy of atomic iodine produced by laser photodissociation. *Phys. Rev. A* **1988**, *38*, 3804–3807.

(40) Nahon, L.; Svensson, A.; Morin, P. Experimental study of the 4 *d* ionization continuum in atomic iodine by photoelectron and photoion spectroscopy. *Phys. Rev. A* **1991**, *43*, 2328–2337.

(41) Holland, D.; Powis, I.; Öhrwall, G.; Karlsson, L.; von Niessen, W. A study of the photoionisation dynamics of chloromethane and iodomethane. *Chem. Phys.* **2006**, *326*, 535–550.

(42) Cooper, J.; Zare, R. N. Angular distribution of photoelectrons. *The Journal of chemical physics* **1968**, *48*, 942–943.

(43) Lindle, D.; Kobrin, P.; Truesdale, C.; Ferrett, T.; Heimann, P.; Kerkhoff, H.; Becker, U.; Shirley, D. Inner-shell photoemission from the iodine atom in CH_3I. *Physical Review A* **1984**, *30*, 239.

(44) Mucke, M.; Zhaunerchyk, V.; Frasinski, L. J.; Squibb, R. J.; Siano, M.; Eland, J. H. D.; Linusson, P.; Salén, P.; Meulen, P. v. d.; Thomas, R. D. et al. Covariance mapping of two-photon double core hole states in C_2H_2 and C_2H_6 produced by an x-ray free electron laser. *New J. Phys.* **2015**, *17*, 073002.

(45) Boschi, R.; Salahub, D. The far ultra-violet spectra of some 1-iodoalkanes. *Molecular Physics* **1972**, *24*, 289–299.

(46) Todt, M. A.; Datta, S.; Rose, A.; Leung, K.; Davis, H. F. Subpicosecond HI elimination in the 266 nm photodissociation of branched iodoalkanes. *Physical Chemistry Chemical Physics* **2020**, *22*, 27338–27347.

(47) Ross, P. L.; Johnston, M. V. Excited state photochemistry of iodoalkanes. *The Journal of Physical Chemistry* **1995**, *99*, 4078–4085.

(48) Mulliken, R. S. Intensities in Molecular Electronic Spectra X. Calculations on Mixed-Halogen, Hydrogen Halide, Alkyl Halide, and Hydroxyl Spectra. *The Journal of Chemical Physics* **1940**, *8*, 382–395.

(49) Chang, K.; Reduzzi, M.; Wang, H. e. a. Revealing electronic state-switching at conical intersections in alkyl iodides by ultrafast XUV transient absorption spectroscopy. *Nat. Commun.* **2020**, *11*, 4042.

(50) Chang, K.; Wang, H.; Marggi Poullain, S.; Prendergast, D.; Neumark, D.; Leone, S. Mapping Wave Packet Bifurcation at a Conical Intersection in CH_3I by Attosecond XUV Transient Absorption Spectroscopy. *ChemRxiv* **2021**,

(51) Lutman, A. A.; MacArthur, J. P.; Ilchen, M.; Lindahl, A. O.; Buck, J.; Coffee, R. N.; Dakovski, G. L.; Dammann, L.; Ding, Y.; Dürr, H. A. et al. Polarization control in an X-ray free-electron laser. *Nature photonics* **2016**, *10*, 468–472.

(52) Duris, J.; Li, S.; Driver, T.; Champenois, E. G.; MacArthur, J. P.; Lutman, A. A.; Zhang, Z.; Rosenberger, P.; Aldrich, J. W.; Coffee, R. et al. Tunable isolated attosecond X-ray pulses with gigawatt peak power from a free-electron laser. *Nat. Photonics* **2020**, *14*, 30–36.

(53) Reiter, F.; Graf, U.; Serebryannikov, E. E.; Schweinberger, W.; Fiess, M.; Schultze, M.; Azzeer, A. M.; Kienberger, R.; Krausz, F.; Zheltikov, A. M. et al. Route to Attosecond Nonlinear Spectroscopy. *Phys. Rev. Lett.* **2010**, *105*, 243902.

(54) Krebs, N.; Pugliesi, I.; Riedle, E. Pulse Compression of Ultrashort UV Pulses by Self-Phase Modulation in Bulk Material. *Applied Sciences* **2013**, *3*, 153–167.

(55) Kobayashi, T.; Kida, Y. Ultrafast spectroscopy with sub-10 fs deep-ultraviolet pulses. *Phys. Chem. Chem. Phys.* **2012**, *14*, 6200–6210.